American Mineralogist, Volume 70, pages 980–986, 1985

Hornblende–cummingtonite and hornblende–actinolite intergrowths from the Koyama calc-alkaline intrusion, Susa, southwest Japan

YOSHIAKI YAMAGUCHI

Department of Geology, Shimane University
Matsue 690, Japan

Abstract

Intergrowth and zoning of interstitial amphiboles in a quartz diorite of the Koyama calc-alkaline intrusion, Susa, southwest Japan indicate that hornblende in this rock initially crystallized in coexistence with cummingtonite, then changed in composition toward actinolite and was ultimately intergrown with hornblende of ferro-hornblende–ferro-actinolitic hornblende composition. The solidus of the interstitial residuum is considered to have crossed the hornblende–cummingtonite and the hornblende–actinolite solvi successively under conditions of high water pressure during the later stages of solidification of the quartz diorite. This suggests a petrogenetic significance of these solvi in controlling crystallization trends for intercumulus amphiboles in hydrous plutonic rocks.

Introduction

Amphibole crystallization plays an essential role in the crystallization sequence of ferromagnesian silicates from hydrous magmas (Wones and Gilbert, 1982). Our knowledge is, however, as yet imperfect on the control of amphibole crystallization trends by solvi, as has been documented for pyroxene and feldspar. Unmixing of hornblende–cummingtonite and hornblende–actinolite is known from many metamorphic rocks (Shido and Miyashiro, 1959; Ross et al., 1969; Klein, 1969; Cooper and Lovering, 1970; Tagiri, 1977; Yamaguchi et al., 1983). Reports of two-amphibole pairs are, however, rare within the igneous environment and are limited to a few cases of hornblende–cummingtonite intergrowths (Klein, 1968; Tomita et al., 1974; Ewart et al., 1975). This report describes intergrowth of hornblende–cummingtonite and hornblende–actinolite in a plutonic rock, and provides evidence indicating a significant role of solvi (Cameron, 1975; Oba, 1980) for amphiboles crystallizing from magma.

Geological setting of amphibole intergrowth

The amphiboles studied occur as interstitial phases, together with quartz, orthoclase, biotite and oxide phases, among early-crystallized plagioclase and pyroxene in a medium-grained quartz diorite of the Koyama calc-alkaline intrusion, Susa, in the San-in area, southwest Japan (Yamazaki, 1967; Honma and Sakai, 1971; Yamaguchi et al., 1974). The intrusion is a small elliptical body (2.0 × 2.4 km), which intrudes sedimentary rocks of Miocene age, converting them to pyroxene hornfels facies at the contact aureole (Suzuki and Nishimura, 1983). The intrusion has a biotite K–Ar age of 11 m.y. (Nishimura et al., 1982). The solidification of the intrusion is believed to have taken place at a maximum pressure of about 1.5 kbar, because the burial depth of the Miocene sedimentary basin in the San-in area is not great (less than 4 km) (Okamoto, 1974; Yamauchi and Yoshitani, 1981).

The intrusion consists of olivine gabbro, anorthositic gabbro, quartz gabbro, quartz diorite, and aplite with gradational contacts. Rhythmic layering is rare and the solidification process was principally controlled by the primary hydrous nature of the magma and by incomplete settling of crystalline phases in the magma chamber. The various rock types in the intrusion were evolved in response to different degrees of accumulation of olivine, pyroxene, and plagioclase in the magma chamber (Yamazaki, 1967). The quartz diorite occurs on the upper border of the intrusion. The amphiboles crystallized in place of pyroxene from residual liquid trapped interstitially in the later stages of solidification of the rock.

Intergrowth textures and chemical analyses of amphiboles

Amphiboles in the quartz diorite developed interstitially with a strongly anhedral form among zoned euhedral plagioclase (An_{85}–An_{23}) and subhedral or anhedral ortho- and clinopyroxene. Pyroxenes are generally corroded at contacts with amphibole. The amphibole is mainly greenish hornblende of hornblende–actinolitic hornblende composition. The greenish hornblende is intergrown with cummingtonite and/or dark greenish hornblende of ferro-hornblende–ferro-actinolitic hornblende composition, as shown by back-scattered electron scanning images and electron microprobe analyses. Back-scattered electron scanning frequently shows exsolution textures between hornblende and cummingtonite and between hornblende and actinolite. Description of the amphibole exsolution phenomena, beyond the purpose of this report, is in preparation.

For two amphibole grains, intergrowth and zoning are discussed below on the bases of electron microprobe analy-

0003–004X/85/0910–0980$02.00

ses and back-scattered electron scanning images using a JXA-50-A microanalyzer. The analytical procedure was previously described (Yamaguchi et al., 1978), and the back-scattered electron scanning images were obtained under 25 kV accelerating voltage and 0.02 μA specimen current. Structural formulae of the amphiboles were calculated on the anhydrous basis of 23 oxygens. A value of $Fe^{3+}/(Fe^{3+} + Fe^{2+}) = 0.16$ is assumed for the greenish hornblendes, based on the data of Yamazaki (1967) who reported three wet chemical analyses of greenish hornblende in the quartz diorite (4.06, 1.63, and 2.80 wt.% Fe_2O_3 and 10.54, 17.56, and 15.06 wt.% FeO, respectively, for a mean $Fe^{3+}/(Fe^{3+} + Fe^{2+})$ value of 0.16). Structural formulae of the dark greenish hornblende were calculated using crystal-chemical constraints according to the method described by Stout (1972) and Robinson et al. (1982). The structural formulae are the means of those calculated by first assuming total cations to be 13 exclusive of K, Na and Ca and then by assuming total cations to be 15 exclusive of K and Na. The calculations yield a range of 0.091–0.114 for $Fe^{3+}/(Fe^{3+} + Fe^{2+})$ in the dark greenish hornblendes. Some problems in applying the calculation methods to the coexisting amphiboles in this study are discussed in a later section.

Hornblende–cummingtonite intergrowth

Figure 1A shows an greenish hornblende of hornblende–actinolitic hornblende composition, enclosing an corroded clinopyroxene grain. The hornblendes is intergrown with cummingtonite. The two phase boundary shows largely smooth but locally irregular form, approximately parallel to common (100). Both amphiboles show a similar greenish color, yet the cummingtonite has a slightly larger extinction angle, 2° on (010). The back-scattered electron scanning image in Figure 1B clearly shows the sharp chemical contrast between the two amphiboles. The textural relation suggests that the greenish hornblende began to form by reaction between clinopyroxene and residual liquid and intergrew with the cummingtonite under a condition at which the solidus extended into the hornblende–cummingtonite solvus. The two amphiboles were shown by microprobe analyses to be chemically homogeneous with no detectable zoning except in narrow areas (10–15 μm thick) adjacent to the contact. Near the contact the greenish hornblende shows a decrease in cummingtonite component with Ca and Al increasing toward the contact; the cummingtonite shows opposite trends. The amphibole analyses are shown in Figure 2 (large and small open squares) by plotting R^{2+} in M4 (where $R^{2+} = Mg + Fe^{2+} + Mn$) and $Fe^{2+}/(Fe^{2+} + Mg)$, respectively, against Al^{IV}. The representative analyses are listed in Table 1. As Figure 2 shows, the two amphiboles in the limited areas near the contact have a larger compositional gap (h–c) in terms of R^{2+} in M4 and Al^{IV} than amphiboles distant from the contact (H–C). This is probably due to subsequent subsolidus reequilibration by solid diffusion across the contact on cooling along the solvus. Their boundary may have been partially reconstructed through the reequilibration, resulting in the present irregular form. Therefore, the compositional difference between the analyses distant from the immediate contact area (H and C in Fig. 2 and Table 1) is considered to represent the miscibility gap during amphibole crystallization at the solidus temperature.

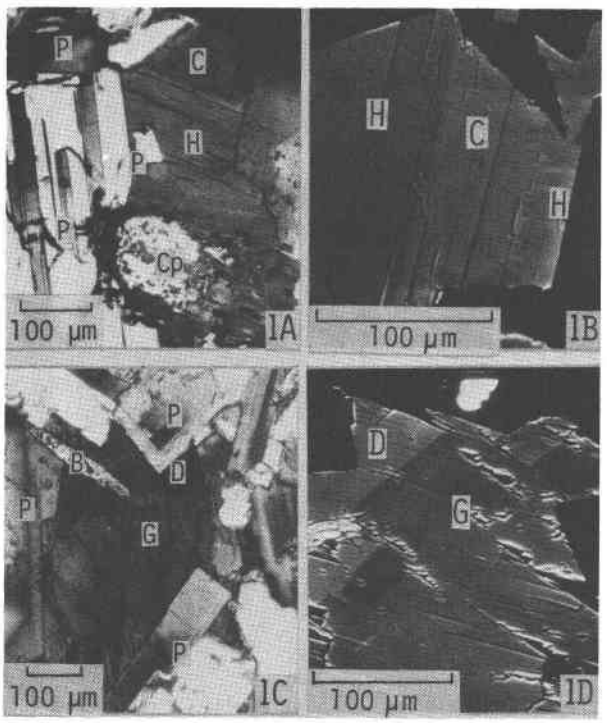

Fig. 1. (A) Greenish hornblende and intergrown cummingtonite. H: greenish hornblende of hornblende–actinolitic hornblende composition, C: cummingtonite, Cp: corroded clinopyroxene, P: plagioclase (polars crossed). (B) Back-scattered electron scanning image of the same amphibole grain. (C) Zoned greenish hornblende and intergrowth of dark greenish hornblende. G: greenish hornblende zoned from hornblende to actinolite, D: dark greenish hornblende of ferro-hornblende–ferro-actinolitic hornblende composition, B: biotite, P: plagioclase (polars crossed). (D) Back-scattered electron scanning image of the same amphibole grain.

In the micrograph of Figure 1B, weak parallel bands of electron density contrast nearly perpendicular to (100) are observed in the top-center. There is, however, no detectable chemical contrast in the microprobe scanning analyses despite each band being sufficiently thick for microprobe resolution. This may be not an exsolution texture but may represent original, very weak oscillatory zoning, though no further evidence is available to confirm this.

Two calcic amphibole intergrowth

The same thin section contains strongly zoned greenish hornblende which is intergrowth with dark greenish hornblende at its rim along sharp contacts. The boundary is shown to be approximately parallel to common $(\bar{1}01)$ by optical observation (Fig. 1C). The back-scattered electron scanning image in Figure 1D clearly resolves the zoning and the intergrowth largely perpendicular to $(\bar{1}01)$. Micro-

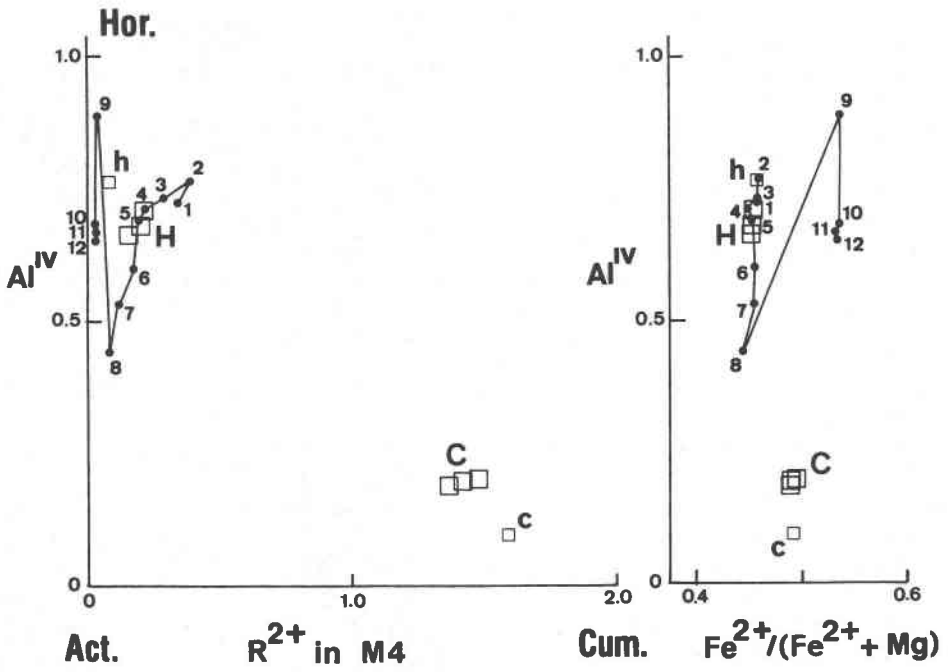

Fig. 2. Chemical compositions of amphiboles, represented by R^{2+} in M4–Al^{IV} and $Fe^{2+}/(Fe^{2+} + Mg)$–Al^{IV} plots, respectively. H and C (large open squares): greenish hornblende and intergrowth cummingtonite, respectively, in Figs. 1A and 1B. h and c (small open squares): reequilibrated compositions of greenish hornblende and cummingtonite, respectively, in areas adjacent to contact of the amphiboles in the same grain. 1–12 (small dots): zoned greenish hornblende and intergrown dark greenish hornblende in Figs. 1C and 1D (analzyed points are shown in Fig. 3A).

probe analyses were made systematically at the points marked in Figure 3A and the resultant analyses are also shown in Figure 2 (small dots). The representative analyses are listed in Table 1. The zoned greenish hornblende changes continuously from hornblende through actinolitic hornblende to actinolite toward its rim and is intergrown with the dark greenish hornblende of ferro-hornblende–ferro-actinolitic hornblende composition. R^{2+} in M4 systematically decreases across the zoning and intergrowth. Al^{IV} decreases continuously in the greenish hornblende and then increases abruptly in the dark greenish hornblende.

There is a surprising compositional break between the two adjoining points across the contact (8 and 9 in Figs. 2 and 3A). Figure 3B shows microprobe scanning profiles for Si and Al across the contact; Si increases and Al decreases toward the contact in the greenish hornblende, while the reverse trends prevail in the dark greenish hornblende. Such compositional fluctuation across the contact zone seems to have resulted from subsolidus reequilibration along the solvus on cooling. Thus, the miscibility gap at the solidus temperature must have been smaller, and may be represented by analyses such as those for points 7 and 10, about 10 μm distant from the contact. The miscibility gap is not so large in Al^{IV} content as that of many metamorphic hornblende–actinolite pairs, yet has a similar break in $Fe^{2+}/(Fe^{2+} + Mg)$ (Tagiri, 1977). This indicates a multidimensional nature of the miscibility gap and suggests that immiscibility in $Si \rightleftarrows Al^{IV}$ substitution, even if small at relatively high-temperature, reflects the strong Mg preference of actinolite during Fe^{2+}–Mg partitioning.

Discussion

Amphibole solid solution among hornblende, cummingonite, and actinolite can be described by four independent substitutions: $Mg \rightleftarrows Fe^{2+}$, $Ca \rightleftarrows Mg$, $MgSi \rightleftarrows (Al^{VI}Fe^{3+})Al^{IV}$ and $Si \rightleftarrows NaAl^{IV}$ (neglecting Ti, Mn, and K). In the quartz diorite, the amphibole crystallization relating

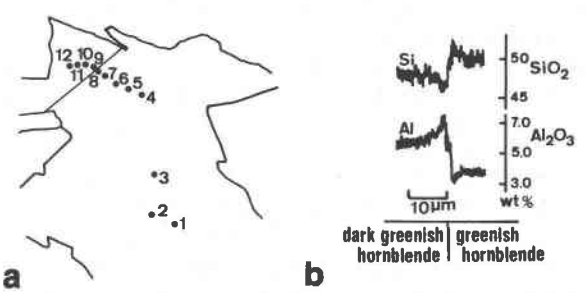

Fig. 3. (A) Analyzed points in the zoned greenish hornblende and dark greenish hornblende intergrowth shown in Figs. 1C and 1D. (B) Microprobe scanning profile of Si and Al across the boundary between the greenish hornblende and dark greenish hornblende.

Table 1. Structural formulae of amphiboles, calculated from representative microprobe analyses, from quartz diorite of the Koyama calc-alkaline intrusion

	H	C	h	c	2	7	8	9	10
SiO_2	49.55	52.51	48.69	53.18	48.94	50.94	51.54	47.08	48.72
TiO_2	0.35	0.11	0.54	0.10	0.38	0.00	0.01	0.11	0.07
Al_2O_3	4.98	1.94	5.70	1.25	4.99	3.97	3.27	7.29	5.57
Fe_2O_3	3.21		3.13		3.46	3.25	3.07	2.67	2.30
FeO	15.16	23.99*	14.81	24.83*	16.35	15.36	14.49	19.37	20.13
MnO	0.37	0.76	0.35	0.67	0.42	0.35	0.30	0.30	0.35
MgO	12.27	14.41	11.51	14.80	12.59	12.28	12.80	8.12	8.40
CaO	10.64	3.43	11.12	2.20	9.78	11.58	11.69	11.86	12.06
Na_2O	0.74	0.28	0.92	0.22	0.89	0.39	0.38	0.58	0.39
K_2O	0.34	0.08	0.45	0.03	0.41	0.14	0.20	0.36	0.26
Total	97.61	97.51	97.22	97.28	98.21	98.26	97.75	97.74	98.25
	Structural formulae based on O = 23								
Si	7.321	7.803	7.237	7.905	7.234	7.468	7.559	7.111	7.319
Al(IV)	0.679	0.197	0.763	0.095	0.766	0.532	0.441	0.889	0.681
Σ(Tet)	8.000	8.000	8.000	8.000	8.000	8.000	8.000	8.000	8.000
Al(VI)	0.188	0.143	0.236	0.125	0.104	0.154	0.125	0.409	0.305
Ti	0.039	0.012	0.060	0.012	0.043	0.000	0.001	0.012	0.008
Fe^{3+}	0.357		0.351		0.385	0.359	0.339	0.303	0.260
Fe^{2+}	1.873	2.981	1.841	3.087	2.022	1.883	1.777	2.447	2.529
Mn	0.046	0.096	0.044	0.084	0.053	0.043	0.037	0.038	0.045
Mg	2.703	3.191	2.550	3.280	2.774	2.684	2.798	1.828	1.881
Σ(Al(VI) to Mg)	5.206	6.423	5.082	6.588	5.381	5.123	5.077	5.037	5.028
R^{2+}** in M4	0.206	1.423	0.082	1.588	0.381	0.123	0.077	0.037	0.028
Ca	1.684	0.545	1.771	0.351	1.548	1.819	1.838	1.919	1.941
Na(M4)	0.110	0.032	0.147	0.061	0.071	0.058	0.085	0.044	0.031
Σ(M4)	2.000	2.000	2.000	2.000	2.000	2.000	2.000	2.000	2.000
Na(A)	0.102	0.048	0.118	0.003	0.185	0.053	0.022	0.126	0.083
K	0.064	0.016	0.085	0.005	0.077	0.026	0.038	0.069	0.050
Σ(A)	0.166	0.064	0.203	0.008	0.262	0.079	0.060	0.195	0.133

* Total Fe as FeO. ** $R^{2+} = Fe^{2+} + Mg + Mn$. Symbols and numbers of analyses are the same as those in Fig. 2.

these three chemically distinct amphiboles can be illustrated by plotting R^{2+} in M4 vs. Al^{IV} and $Fe^{2+}/(Fe^{2+} + Mg)$ vs. Al^{IV} as shown in Figure 2. In calculating the structural formulae, the method based on normalizing cation occupancy in the amphibole M4 site (Stout, 1972; Robinson et al., 1982) was not suitable for the greenish hornblende. Generally, calcic amphibole coexisting with cummingtonite is believed to have a substantially large number of R^{2+} cations in M4, substituting for Ca + Na, due to a relatively large cummingtonite component in solid solution (Ross et al., 1969). The greenish hornblendes recalculate to the unlikely large values of $Fe^{3+}/(Fe^{3+} + Fe^{2+}) = 0.29$ to 0.72 on the assumption of 13 cations, exclusive of K, Na, and Ca (i.e. eliminating the cummingtonite component). The assumption of 15 cations, exclusive of K and Na, yields $Fe^{3+}/(Fe^{3+} + Fe^{2+}) = 0.046$ to 0.10. The means of the $Fe^{3+}/(Fe^{3+} + Fe^{2+})$ values calculated assuming 13 cations are strongly variable, changing from 0.12 to 0.39 as Ca content decreases; the average for all the greenish hornblende analyses is 0.26. Such a high $Fe^{3+}/(Fe^{3+} + Fe^{2+})$ value is not consistent with the average value, 0.16, obtained from the wet chemical data. On the other hand, the value 0.16 is not suitable for $Fe^{3+}/(Fe^{3+} + Fe^{2+})$ in the dark greenish hornblendes, because their structural formulae calculated using this value give total cation numbers that are too low for appropriate amphibole structural formulae and involve unreasonable assignment of Ca to M1–M3 (0.002–0.025 cations).

In fact, it is not conceivable that the same $Fe^{3+}/(Fe^{3+} + Fe^{2+})$ is characteristic of the two distinct calcic amphibole solid solutions. During early amphibole crystallization, the relatively low Ca content of the greenish hornblende, coexisting with cummingtonite, is essentially due to substitution of cummingtonite component, rather

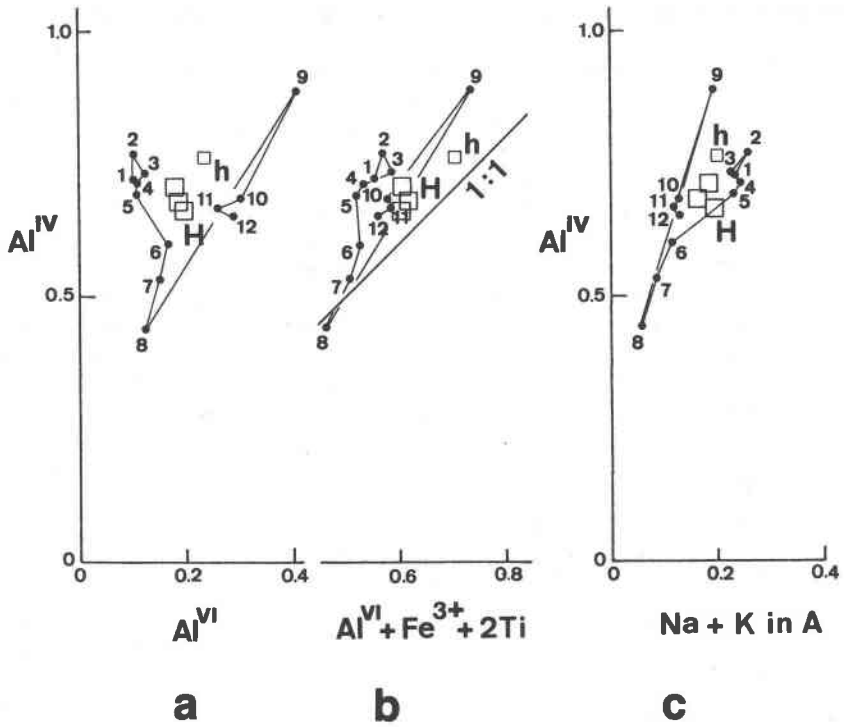

Fig. 4. Plots of (a) Al^{VI}–Al^{IV}, (b) ($Al^{VI} + Fe^{3+} + 2Ti$)–Al^{IV}, and (c) (Na + K) in A site–Al^{IV}, respectively. Symbols and numbers identifying analyses are the same as those in Figs. 2 and 3A.

than sodic amphibole component involving high Fe^{3+}. This is supported by evidence that the hornblende increased in Ca content on cooling during later subsolidus reequilibration.

Coupled substitutions operative in the calcic amphiboles are shown in Figures 3A, 3B, and 3C, in which Al^{VI}, $Al^{VI} + Fe^{3+} + 2Ti$, and Na + K in the A site are plotted, respectively, against Al^{IV}. As Figure 3B shows, substitution of Al^{IV} for Si in the calcic amphiboles is dominantly compensated by substitution of Al^{VI}, Fe^{3+}, and Ti in octahedral sites. A-site occupancy of Na and K should be balanced mainly by the remaining deficient tetrahedral charge and partly by substitution of Na for Ca in M4, as shown by the contrast between Figures 3B and 3C. Figure 3A shows that there is a characteristically small Al^{VI} content in the calcic amphiboles. Thus, Fe^{3+} is the dominant octahedral trivalent cation in the greenish hornblende, and Fe^{3+} constitutes approximately half the summed charge of $Al^{VI} + Fe^{3+} + 2Ti$ in the dark greenish hornblendes. The characteristic features of cation substitution described above are essentially similar to those found in calcic amphiboles from the Finnmarka complex, Norway and in magnetite-series granitoids in the inner zone batholith of southwestern Japan (Czamanske and Wones, 1973; Czamanske et al., 1981; Kanisawa, 1983).

The zoning and intergrowth described here record a history of calcic amphibole crystallization. Crystallization was initially constrained by the hornblende–cummingtonite solvus; then, during cooling of the residual magma, hornblende changed in composition toward actinolite with the cummingtonite component decreasing along the solvus. With further decrease in temperature, hornblende composition finally reached $Al^{IV} \simeq 0.5$, at which point hornblende terminated hyper-solvus crystallization beyond the hornblende–actinolite solvus, and began to intergrow with the dark greenish hornblende of ferro-hornblende–ferro-actinolitic hornblende composition.

Zoning of the greenish hornblende toward actinolite involves no increase in $Fe^{2+}/(Fe^{2+} + Mg)$ (Fig. 2). Total Fe in the greenish hornblende decreases slightly toward the rim from 2.41 to 2.24 cations (analytical points 2→7, Table 1). Calcic amphibole crystallization involving constant or decreasing $Fe^{2+}/(Fe^{2+} + Mg)$ as the magma evolved toward a siliceous residuum has been described from some plutonic rocks and is interpreted to reflect increasing oxygen fugacity in the magma (Czamanske and Wones, 1973; Mason, 1978; Czamanske et al., 1981; Chivas, 1981). Yamazaki (1967) pointed out that the interstitial phases of the quartz diorite crystallized under high oxygen fugacity in association with magnetite containing much hematite in solid solution. Contrasting high $Fe^{2+}/(Fe^{2+} + Mg)$ in the intergrown dark greenish hornblende must be ascribed to strong Fe preference by hornblende of the hornblende–actinolite solvus (Tagiri, 1977).

No evidence suggests increase of oxygen fugacity in the later stages of amphibole crystallization.

Hornblende–cummingtonite pairs are known in rocks ranging from epidote amphibolite facies metamorphic rocks to rhyolites (725–750°C) (Ewart et al., 1975). An experimental study by Oba (1980) showed that the miscibility gap of calcic amphibole is extended to approximately 825°C at 1 kbar P_{H_2O} in the system tremolite–pargasite. Oba showed that the solvus is strongly depressed by addition of Fe to this pure binary system and by increasing pressure. The crest of the hornblende–actinolite solvus in metamorphic rocks is estimated to lie between 500° and 700°C (Hietanen, 1974; Misch and Rice, 1975; Spear, 1980). Because the amphiboles in the Koyama intrusion crystallized at a shallow level, the solvus may not have been much depressed. Because there was no iron-enrichment in calcic amphibole crystallization toward actinolite, this solvus is thought to have been prevented from depression even as the magma was evolving toward a siliceous residuum. The solidus of the interstitial magma is considered to have crossed this solvus under a condition of high water pressure during the later stages of solidification. Volatiles such as HF, NaF, and Li_2O, that are expected to have been enriched in the residuum, might have lowered the solidus temperature (Jahns and Burnham, 1958; Wyllie and Tuttle, 1961). It is believed that the unmixing phenomena described here will, through careful observation, be found widely in intercumulus amphiboles in plutonic rocks which were intruded to shallow level and crystallized under conditions of high oxygen fugacity and high water pressure.

Acknowledgments

I am grateful to Katsutoshi Tomita, Yoshihiro Sawada and Hideo Kobayashi for helpful discussion and Kenzo Yagi, A. F. Cooper, S. O. Agrell, Shigeru Iizumi, Teruo Watanabe and Yasuyuki Miyake for advice and for reading the manuscript in an early stage. Kenzo Yagi improved the final manuscript.

References

Cameron, K. L. (1975) An experimental study of actinolite–cummingtonite phase relations with notes on the synthesis of Fe-rich anthopyllite. American Mineralogist, 60, 375–390.

Chivas, A. R. (1981) Geochemical evidence for magmatic fluids in porphyry copper mineralization. Part 1. Mafic silicates from the Koloula igneous complex. Contributions to Mineralogy and Petrology, 78, 389–403.

Cooper, A. F. and Lovering, J. F. (1970) Greenschist amphiboles from Haast River, New Zealand. Contributions to Mineralogy and Petrology, 27, 11–24.

Czamanske, G. K. and Wones, D. R. (1973). Oxidation during magmatic differentiation, Finnmarka Complex, Oslo area, Norway: Part 2, The mafic silicates. Journal of Petrology, 14, 349–380.

Czamanske, G. K., Ishihara, S. and Atkin, S. A. (1981) Chemistry of rock-forming minerals of the Cretaceous–Paleogene batholith in southwestern Japan and implications for magma genesis. Journal of Geophysical Research, 86, 10431–10469.

Ewart, A., Hildreth, W. and Carmichael, I. S. E. (1975) Quaternary acid magma in New Zealand. Contributions to Mineralogy and Petrology, 51, 1–27.

Hietanen, A. (1974) Amphibole pairs, epidote minerals, chlorite and plagioclase in metamorphic rocks, northern Sierra Nevada, California. American Mineralogist, 59, 22–40.

Honma, H. and Sakai, H. (1971) Oxygen isotope study of the Koyama intrusive complex, Yamaguchi Prefecture, southwest Japan. Geochemical Journal, 4, 93–103.

Jahns, R. H. and Burnham, C. W. (1958) Experimental studies of pegmatite genesis: Part 2, Melting and recrystallization of granite and pegmatite (abstr.). Geological Society of America Bulletin, 69, 1592–1593.

Kanisawa, S. (1983) Chemical characteristics of biotites and hornblendes of late Mesozoic to early Tertiary granitic rocks in Japan. Geological Society of America Memoir, 159, 129–134.

Klein, C. (1968) Coexisting amphiboles. Journal of Petrology, 9, 281–330.

Klein, C. (1969) Two-amphibole assemblages in the system actinolite–hornblende–glaucophane. American Mineralogist, 54, 212–237.

Mason, D. R. (1978) Compositional variations in ferromagnesian minerals from porphyry copper-generating and barren intrusions of the Western Highlands, Papua New Guinea. Economic Geology, 73, 878–890.

Misch, P. and Rice, J. M. (1975) Miscibility of tremolite and hornblende in progressive Skagit metamorphic suite, North Cascades, Washington. Journal of Petrology, 16, 1–21.

Nishimura, Y., Suzuki, M. and Nakamura, E. (1982) Contact metamorphic rocks and its K–Ar age in the Susa-Koyama area (in Japanese). Reports of Nishinihon Branch of Geological Society of Japan, 74, 14–15.

Oba, T. (1980) Phase relations in the tremolite–pargasite join. Contributions to Mineralogy and Petrology, 71, 247–256.

Okamoto, K. (1974) Tertiary systems in western San-in (in Japanese). Chishitsu News (ed. Geological Survey of Japan), No. 243, 12–21 (Jitsugyokoho, Inc.).

Robinson, P., Spear, F. S., Schumacher, J. C., Laird, J., Klein, C., Evans, B. W. and Doolan, B. L. (1982) Phase relations of metamorphic amphiboles: Natural occurrence and theory. In D. R. Veblen and P. H. Ribbe, Reviews in Mineralogy 9B. Amphiboles: Petrology and experimental phase relations 1–227. Mineralogical Society of America, Washington, D.C.

Ross, M., Papike, J. J. and Shaw, K. W. (1969) Exsolution textures in amphiboles as indicators of subsolidus thermal histories. Mineralogical Society of America Special Publication, No. 2, 275–299.

Shido, F. and Miyashiro, A. (1959) Hornblendes of the basic metamorphic rocks. Journal of the Faculty of Science University of Tokyo, Sec. 2, 12, 85–102.

Spear, F. S. (1980) NaSi ⇄ CaAl exchange equilibrium between plagioclase and amphibole. Contributions to Mineralogy and Petrology, 72, 33–41.

Stout, J. H. (1972) Phase petrology and mineral chemistry of coexisting amphiboles from Telemark, Norway. Journal of Petrology, 13, 99–145.

Suzuki, M. and Nishimura, Y. (1983) Contact metamorphic effect on basaltic rocks by the Koyama gabbro complex, Susa area, southwest Japan. Journal of Science of the Hiroshima University, ser. C, 8, No. 2, 149–163.

Tagiri, M. (1977) Fe–Mg partition and miscibility gap between coexisting calcic amphiboles from the southern Abukuma plateau, Japan. Contributions to Mineralogy and Petrology, 62, 271–281.

Tomita, K., Yamaguchi, Y. and Takita, R. (1974) Exsolution texture in coexisting amphiboles from Tanzawa tonalite complex,

Tanzawa mountainland, central Japan. Memoirs of the Geological Society of Japan, No. 11, 95–106.

Wones, D. R. and Gilbert, M. C. (1982) Amphiboles in the igneous environment. In D. R. Veblen and P. H. Ribbe, Reviews in Mineralogy 9B. Amphiboles: Petrology and experimental phase relations p. 355–390. Mineralogical Society of America, Washington, D.C.

Wyllie, P. J. and Tuttle, O. F. (1961) Experimental investigation of silicate systems containing two volatile components: Part 2. American Journal of Science, 259, 128–143.

Yamaguchi, Y., Tomita, K. and Sawada, Y. (1974) Crystallization trend of zoned pyroxenes in quartz gabbro from the Koyama intrusive complex at Mt. Koyama, Yamaguchi prefecture, Japan. Memoirs of the Geological Society of Japan, No. 11, 69–82.

Yamaguchi, Y., Akai, J. and Tomita, K. (1978) Clinoamphibole lamellae in diopside of garnet lherzolite from Alpe Arami, Bellinzona, Switzerland. Contributions to Mineralogy and Petrology, 66, 263–270.

Yamaguchi, Y., Shibakusa, H. and Tomita, K. (1983) Exsolution of cummingtonite, actinolite and sodic amphibole in hornblende in high-pressure metamorphism. Nature, 304, No. 5923, 257–259.

Yamaguchi, S. and Yoshitani, A. (1981) Tectonic movements in the progressive stage of the Green-tuff basins—Taking the case of the Miocene series in the eastern part of Shimane prefecture, western Japan (in Japanese with English abstract). Journal of the Geological Society of Japan, 87, No. 11, 711–724.

Yamazaki, T. (1967) Petrology of the Koyama calc-alkaline intrusive complex, Yamaguchi prefecture, Japan. Science Reports of the Tohoku University, ser. 3, 10, 99–150.

Manuscript received, April 26, 1984;
accepted for publication, April 23, 1985.